Scientific Research Publishing

International Journal of Astronomy and Astrophysics, 2024, 14, 101-119
https://www.scirp.org/journal/ijaa
ISSN Online: 2161-4725
ISSN Print: 2161-4717

New Probability Distributions in Astrophysics: XII. Truncation for the Gompertz Distribution

Lorenzo Zaninetti

Physics Department, University of Turin, Turin, Italy
Email: l.zaninetti@alice.it

How to cite this paper: Zaninetti, L. (2024) New Probability Distributions in Astrophysics: XII. Truncation for the Gompertz Distribution. *International Journal of Astronomy and Astrophysics*, **14**, 101-119.
https://doi.org/10.4236/ijaa.2024.142007

Received: April 20, 2024
Accepted: June 14, 2024
Published: June 17, 2024

Abstract

Analytical functions which fit the probability distributions of stars and galaxies can provide insight into how these distributions originate. In order to introduce a truncated version of the Gompertz distribution, we derive its probability density function, its distribution function, its average value, its second moment about the origin, its median, its random generation of values and a maximum likelihood estimator for its two unknown parameters. The astrophysical applications of the Gompertz distribution are the initial mass function for stars, the luminosity function for the galaxies of the Sloan Digital Sky Survey, the photometric maximum of galaxies visible in the GLADE+ catalog and a model for the mean absolute magnitude in the GLADE+ catalog as a function of the redshift.

Keywords

Stars: Normal, Stars: Luminosity Function, Mass Function Stars: Statistics

1. Introduction

The Gompertz distribution [1], taking values in the interval from zero to infinity, is a continuous probability distribution that has an exponentially increasing failure rate. The death rate of adult humans increases exponentially, so the Gompertz distribution is widely used in actuarial science. We now outline some applications in physics. The phenomenon of the oscillatory behavior of the counting statistics observed in high energy experimental data is explained by the the shifted Gompertz distribution [2]. There is a two-component model in which a probability distribution function obtained from the superposition of two shifted Gompertz distributions explains the multiplicity distributions of charged particles produced in $e^+ - e^-$ collisions at the LEP, pp interactions at the SPS and pp collisions at the LHC at different centers of mass energies in full phase

space as well as in restricted phase space [3] [4]. The shifted Gompertz distribution was used in order to explain the modified multiplicity distributions in four different types of neutrino-induced interaction [5]. At the moment of writing, the Gompertz distribution in astrophysics is unknown and therefore some questions arise.

- Can the Gompertz distribution model the initial mass function for stars?
- Can the Gompertz distribution model the luminosity function for galaxies?
- Is using the truncated Gompertz distribution better than using the untruncated one?

In order to answer the above questions, Section 2 treats the untruncated Gompertz distribution and Section 3 introduces its truncation. Section 4 applies the obtained results to the initial mass function for stars. Section 5 derives the untruncated and truncated Gompertz luminosity function for galaxies, parameterizes the photometric maximum for the number of galaxies as a function of the redshift and models the mean absolute magnitude of galaxies as a function of the redshift.

2. The Gompertz Distribution

The *Gompertz* probability density function (PDF) is

$$f(x)=a\mathrm{e}^{bx-\frac{a\left(\mathrm{e}^{bx}-1\right)}{b}}, \tag{1}$$

for $0\le x\le\infty$, which at $x=0$ takes the value a, see [6] [7]. The distribution function (DF) of the Gompertz distribution is

$$F(x;a,b)=1-\mathrm{e}^{-\frac{a\left(\mathrm{e}^{bx}-1\right)}{b}}, \tag{2}$$

and its average value or mean, μ, is

$$\mu(a,b)=\frac{\mathrm{e}^{\frac{a}{b}}\mathrm{Ei}_1\left(\frac{a}{b}\right)}{b}, \tag{3}$$

see formulae (A.1) for the definition of $\mathrm{Ei}_a(z)$ in the Appendix. The moment generating function $m(t;a,b)$ is given by

$$m(t;a,b)=\mathrm{e}^{\frac{a}{b}}b^{\frac{t}{b}}\Gamma\left(\frac{t+b}{b},\frac{a}{b}\right)a^{-\frac{t}{b}}, \tag{4}$$

where the incomplete Gamma function is defined by Equation (A.3). The moment generating function allows deriving the second moment about the origin $m(a,b)_2'$

$$m(a,b)_2'=\frac{1}{6b^3}\left[-\left(-\pi^2b-6\gamma^2b-12\ln\left(\frac{a}{b}\right)\gamma b-6\ln\left(\frac{a}{b}\right)^2b+12{}_3F_3\left(1,1,1;2,2,2;-\frac{a}{b}\right)a\right)\mathrm{e}^{\frac{a}{b}}\right], \tag{5}$$

where γ is the Euler-Mascheroni constant, see the definition in Equation

(A.10), Equations (A.5) and (A.7) define the generalized hypergeometric function in the particular case here used. The third moment $m(a,b)_3'$ about the origin is

$$m(a,b)_3' = \frac{1}{2b^4}\left[-\left(\gamma\pi^2 b + \ln\left(\frac{a}{b}\right)\pi^2 b + 2\gamma^3 b + 6\ln\left(\frac{a}{b}\right)\gamma^2 b + 6\ln\left(\frac{a}{b}\right)^2 \gamma b + 2\ln\left(\frac{a}{b}\right)^3 b + 4\zeta(3)b - 12\,{}_4F_4\left(1,1,1,1;2,2,2,2;-\frac{a}{b}\right)a\right)e^{\frac{a}{b}}\right], \tag{6}$$

where ${}_4F_4(1,1,1,1;2,2,2,2;z)$ has a power law expansion as given by Equation (A.8) and the Riemann zeta function, $\zeta(z)$, is defined by Equation (A.11).

The fourth moment about the origin $m(a,b)_4'$ is

$$m(a,b)_4' = \frac{1}{20b^5}\left[\left(20b\gamma^4 + 80\ln\left(\frac{a}{b}\right)\gamma^3 b + 20b\pi^2\gamma^2 + 120\ln\left(\frac{a}{b}\right)^2\gamma^2 b + 40\ln\left(\frac{a}{b}\right)\gamma\pi^2 b + 80\ln\left(\frac{a}{b}\right)^3\gamma b + 3b\pi^4 + 20\ln\left(\frac{a}{b}\right)^2\pi^2 b + 20\ln\left(\frac{a}{b}\right)^4 b + 160b\zeta(3)\gamma + 160\ln\left(\frac{a}{b}\right)\zeta(3)b - 480\,{}_5F_5\left(1,1,1,1,1;2,2,2,2,2;-\frac{a}{b}\right)a\right)e^{\frac{a}{b}}\right], \tag{7}$$

where ${}_5F_5(1,1,1,1,1;2,2,2,2,2;z)$ is defined in Equation (A.9). The variance can be evaluated with the usual formula

$$\sigma^2(a,b) = m(a,b)_2' - \mu(a,b)^2, \tag{8}$$

and is

$$\sigma^2(a,b) = \frac{1}{6b^3}\left[-e^{\frac{a}{b}}\left(6e^{\frac{a}{b}}\mathrm{Ei}_1\left(\frac{a}{b}\right)^2 b - \pi^2 b - 6\gamma^2 b - 12\ln\left(\frac{a}{b}\right)\gamma b - 6\ln\left(\frac{a}{b}\right)^2 b + 12\,{}_3F_3\left(1,1,1;2,2,2;-\frac{a}{b}\right)a\right)\right]. \tag{9}$$

The same result for the variance can be found in the formula after (15) in [6] or the formula after (16) in [7]. The skewness and the kurtosis have complicated expressions and we omit them. The random generation of the Gompertz variate X is given by

$$X : a,b \approx \frac{-\ln(a) + \ln\left(-\ln(1-R)b + a\right)}{b}, \tag{10}$$

where R is the unit rectangular variate. The median, $q_{1/2}$, is at

$$q_{1/2}(a,b) = \frac{-\ln(a) + \ln\left(\ln(2)b + a\right)}{b}. \tag{11}$$

The mode is at

$$\mathrm{mode}(a,b) = \frac{\ln\left(\frac{b}{a}\right)}{b}, \tag{12}$$

and is defined to be positive for $b > a$. The first method to find the two parameters a and b is given by the maximum likelihood estimator (MLE) which solves numerically the two following equations

$$\frac{1}{ab}\left[-\left(\sum_{i=1}^{n} e^{bx_i}\right)a + na + nb\right] = 0, \tag{13}$$

$$\frac{1}{b^2}\left[-na - \sum_{i=1}^{n}\left(a\left(bx_i - 1\right)e^{bx_i} - b^2 x_i\right)\right] = 0. \tag{14}$$

The second method to determine the parameters is to introduce the moments of the experimental sample

$$\overline{x}_r = \frac{1}{n}\sum_{i}^{n} x_i^r. \tag{15}$$

As a consequence, the two parameters can be found by solving the following two non-linear equations, the method of moments (MOM)

$$\overline{x}_1 = \mu(a,b), \tag{16}$$

$$\overline{x}_2 = m(a,b)_2'. \tag{17}$$

3. Truncated Gompertz Distribution

The DF of the truncated Gompertz distribution, $F_T(x)$, is

$$F_T(x;a,b,x_l,x_u) = -\left(e^{\frac{a\left(e^{bx}-e^{bx_l}+1\right)}{b}} - e^{\frac{a}{b}}\right)e^{-\frac{ae^{bx}}{b}}, \tag{18}$$

and its PDF, $f_T(x)$, is

$$f_T(x;a,b,x_l,x_u) = -\frac{ae^{\frac{b^2x - ae^{bx} + a}{b}}}{e^{-\frac{a\left(e^{bx_u}-1\right)}{b}} - e^{-\frac{a\left(e^{bx_l}-1\right)}{b}}}. \tag{19}$$

Its variate X will be a random variable taking values in $[x_l, x_u]$. Its average value or mean, μ_T, is

$$\mu_T(a,b,x_l,x_u) = \frac{1}{b\left(e^{-\frac{a\left(e^{bx_u}-1\right)}{b}} - e^{-\frac{a\left(e^{bx_l}-1\right)}{b}}\right)}\left[bx_u e^{-\frac{a\left(e^{bx_u}-1\right)}{b}} - e^{-\frac{a\left(e^{bx_l}-1\right)}{b}}x_l b - e^{\frac{a}{b}}\mathrm{Ei}_1\left(\frac{ae^{bx_l}}{b}\right) + e^{\frac{a}{b}}\mathrm{Ei}_1\left(\frac{ae^{bx_u}}{b}\right)\right]. \tag{20}$$

The second moment about the origin $m(a,b,x_l,x_u)_{2,T}'$ is

$$m(a,b,x_l,x_u)_{2,T}' = \frac{1}{b^3\left(e^{-\frac{a\left(e^{bx_u}-1\right)}{b}} - e^{-\frac{a\left(e^{bx_l}-1\right)}{b}}\right)}\left[e^{\frac{a}{b}}\left(-b^3 e^{-\frac{ae^{bx_l}}{b}}x_l^2 + b^3 e^{-\frac{ae^{bx_u}}{b}}x_u^2 - b^3 x_l^2\right)\right. \tag{21}$$

$$+b^3x_u^2-2b^2\mathrm{Ei}_1\left(\frac{a\mathrm{e}^{bx_l}}{b}\right)x_l+2b^2\mathrm{Ei}_1\left(\frac{a\mathrm{e}^{bx_u}}{b}\right)x_u-2b^2\ln(a)x_l+2b^2\ln(a)x_u$$

$$+2b^2\ln(b)x_l-2b^2\ln(b)x_u-2b^2\gamma x_l+2b^2\gamma x_u+2\,{}_3F_3\left(1,1,1;2,2,2;-\frac{a\mathrm{e}^{bx_l}}{b}\right)\mathrm{e}^{bx_l}a$$

$$-2\,{}_3F_3\left(1,1,1;2,2,2;-\frac{a\mathrm{e}^{bx_u}}{b}\right)\mathrm{e}^{bx_u}a\Bigg]. \tag{22}$$

The variance can be evaluated by

$$\sigma_T^2(a,b,x_l,x_u)=m(a,b,x_l,x_u)'_{2,T}-\mu_T(a,b,x_l,x_u)^2. \tag{23}$$

The random generation of the variate X of the truncated Gompertz is

$$X:a,b,x_l,x_u\approx\frac{1}{b}\left[-\ln(a)+\ln\left(\ln\left(\frac{1}{(-R+1)\mathrm{e}^{\frac{a\left(\mathrm{e}^{bx_u}-1\right)}{b}}+R\mathrm{e}^{\frac{a\left(\mathrm{e}^{bx_l}-1\right)}{b}}}\right)b+\left(\mathrm{e}^{bx_u}+\mathrm{e}^{bx_l}-1\right)a\right)\right]. \tag{24}$$

The median is

$$q_{1/2}(a,b,x_l,x_u)_T=\frac{1}{b}\left[-\ln(a)+\ln\left(b\ln(2)-b\ln\left(\mathrm{e}^{\frac{a\left(\mathrm{e}^{bx_u}-1\right)}{b}}+\mathrm{e}^{\frac{a\left(\mathrm{e}^{bx_l}-1\right)}{b}}\right)+a\mathrm{e}^{bx_l}+a\mathrm{e}^{bx_u}-a\right)\right]. \tag{25}$$

The four parameters x_l, x_u, a and b can be obtained in the following way. Consider a sample $\mathcal{X}=x_1,x_2,\cdots,x_n$ and let $x_{(1)}\geq x_{(2)}\geq\cdots\geq x_{(n)}$ denote their order statistics, so that $x_{(1)}=\max(x_1,x_2,\cdots,x_n)$, $x_{(n)}=\min(x_1,x_2,\cdots,x_n)$. The two parameters x_l and x_u are

$$x_l=x_{(n)};\quad x_u=x_{(1)}. \tag{26}$$

The two remaining parameters a and b are found by solving the two following equations which arise from the MLE

$$\frac{1}{ab\left(\mathrm{e}^{-\frac{a\left(\mathrm{e}^{bx_u}-1\right)}{b}}-\mathrm{e}^{-\frac{a\left(\mathrm{e}^{bx_l}-1\right)}{b}}\right)}\left[-\left(\sum_{i=1}^{n}\mathrm{e}^{bx_i}\right)\mathrm{e}^{-\frac{a\left(\mathrm{e}^{bx_u}-1\right)}{b}}a+\left(\sum_{i=1}^{n}\mathrm{e}^{bx_i}\right)\mathrm{e}^{-\frac{a\left(\mathrm{e}^{bx_l}-1\right)}{b}}a\right.$$
$$\left.-an\mathrm{e}^{-\frac{a\left(\mathrm{e}^{bx_l}-1\right)}{b}+bx_l}+an\mathrm{e}^{-\frac{a\left(\mathrm{e}^{bx_u}-1\right)}{b}+bx_u}+\mathrm{e}^{-\frac{a\left(\mathrm{e}^{bx_u}-1\right)}{b}}bn-\mathrm{e}^{-\frac{a\left(\mathrm{e}^{bx_l}-1\right)}{b}}bn\right]=0, \tag{27}$$

and

$$\frac{1}{\left(\mathrm{e}^{-\frac{a\left(\mathrm{e}^{bx_u}-1\right)}{b}}-\mathrm{e}^{-\frac{a\left(\mathrm{e}^{bx_l}-1\right)}{b}}\right)b^2}\left[-\mathrm{e}^{-\frac{a\left(\mathrm{e}^{bx_l}-1\right)}{b}+bx_l}abnx_l+\mathrm{e}^{-\frac{a\left(\mathrm{e}^{bx_u}-1\right)}{b}+bx_u}abnx_u\right.$$
$$\left.+an\mathrm{e}^{-\frac{a\left(\mathrm{e}^{bx_l}-1\right)}{b}+bx_l}-an\mathrm{e}^{-\frac{a\left(\mathrm{e}^{bx_u}-1\right)}{b}+bx_u}-\left(\sum_{i=1}^{n}\left(a(bx_i-1)\mathrm{e}^{bx_i}-b^2x_i\right)\right)\mathrm{e}^{-\frac{a\left(\mathrm{e}^{bx_u}-1\right)}{b}}\right. \tag{28}$$

$$+\left(\sum_{i=1}^{n}\left(a\left(bx_i-1\right)\mathrm{e}^{bx_i}-b^2x_i\right)\right)\mathrm{e}^{-\frac{a\left(\mathrm{e}^{bx_i}-1\right)}{b}}\Bigg]=0,$$

where x_i are the elements of the experimental sample with i varying between 1 and n. A second method to determine a and b is the MOM method, see Equations (16) and (17).

4. Application to the Stars

4.1. Statistics

The merit function χ^2 is computed according to the formula

$$\chi^2=\sum_{i=1}^{n}\frac{\left(T_i-O_i\right)^2}{T_i}, \tag{29}$$

where n is the number of bins, T_i is the theoretical value, and O_i is the experimental value represented by the frequencies. The theoretical frequency distribution is given by

$$T_i=N\Delta x_i\,p\left(x\right), \tag{30}$$

where N is the number of elements of the sample, Δx_i is the magnitude of the size interval, and $p\left(x\right)$ is the PDF under examination. A reduced merit function χ^2_{red} is given by

$$\chi^2_{red}=\chi^2/NF, \tag{31}$$

where $NF=n-k$ is the number of degrees of freedom, n is the number of bins, and k is the number of parameters. The goodness of the fit can be expressed by the probability Q, see equation 15.2.12 in [8], which involves the number of degrees of freedom and χ^2. According to [8] p. 658, the fit "may be acceptable" if $Q>0.001$. The Akaike information criterion (AIC), see [9], is defined by

$$\mathrm{AIC}=2k-2\ln\left(L\right), \tag{32}$$

where L is the likelihood function and k the number of free parameters in the model. We assume a Gaussian distribution for the errors. The likelihood function can then be derived from the χ^2 statistic $L\propto\exp\left(-\frac{\chi^2}{2}\right)$ where χ^2 has been computed by Equation (29), see [10] [11]. Now the AIC becomes

$$\mathrm{AIC}=2k+\chi^2. \tag{33}$$

The Kolmogorov--Smirnov test (K--S), see [12] [13] [14], does not require the data to be binned. The K--S test, as implemented by the FORTRAN subroutine KSONE in [8], finds the maximum distance, D, between the theoretical and the astronomical DFs, as well as the significance level P_{KS}, see formulas 14.3.5 and 14.3.9 in [8]. If $P_{KS}\geq 0.1$, then the goodness of the fit is believable.

4.2. The IMF for Stars

The first test is performed on NGC 2362, where the 271 stars have a range of

$1.47M_{\odot} \geq M \geq 0.11M_{\odot}$, see [15] and CDS catalog J/MNRAS/384/675/table1. According to [16], the distance of NGC 2362 is 1480 pc. The second test is performed on the low-mass IMF in the young cluster NGC 6611, see [17] and CDS catalog J/MNRAS/392/1034. This massive cluster has an age of 2 - 3 Myr and contains masses from $1.5M_{\odot} \geq M \geq 0.02M_{\odot}$. Therefore, the brown dwarf (BD) region, $\approx 0.2\mathcal{M}_{\odot}$, is covered. The third test is performed on the γ Velorum cluster where the 237 stars have a range of $1.31M_{\odot} \geq M \geq 0.15M_{\odot}$, see [18] and CDS catalog J/A+A/589/A70/table5. The fourth test is performed on the young cluster Berkeley 59, where the 420 stars have a range of $2.24M_{\odot} \geq M \geq 0.15M_{\odot}$, see [19] and CDS catalog J/AJ/155/44/table3. The results are presented in **Table 1** for the Gompertz distribution, and in **Table 2** for the truncated Gompertz distribution. In **Table 1** and **Table 2** the last column shows whether the results of the K--S test are better when compared to the lognormal distribution (Y) or worse (N).

As an example, the empirical DF visualized through histograms and the theoretical Gompertz DF for NGC 2362 is presented in **Figure 1**.

Another example is given by the PDF of the truncated Gompertz distribution, see **Figure 2**.

Table 1. Numerical values of χ^2_{red}, AIC, probability Q, D, the maximum distance between theoretical and observed DFs, and P_{KS}, the significance level, in the K--S test of the Gompertz distribution, see Equation (1), for different astrophysical environments. The last column (F) indicates a P_{KS} higher (Y) or lower (N) than that for the lognormal distribution. The number of linear bins, n, is 10.

Cluster	parameters	AIC	χ^2_{red}	Q	D	P_{KS}	F
NGC 2362	$a = 0.379$, $b = 2.759$	18.34	1.793	7.31×10^{-2}	6.89×10^{-2}	0.145	Y
NGC 6611	$a = 1.613$, $b = 0.988$	9.313	0.664	0.723	5.84×10^{-2}	0.468	Y
γ Velorum	$a = 1.533$, $b = 1.6$	135	16.37	0	0.24	1.42×10^{-12}	N
Berkeley 59	$a = 2.375$, $b = 0.349$	125.16	15.145	0	0.373	0	N

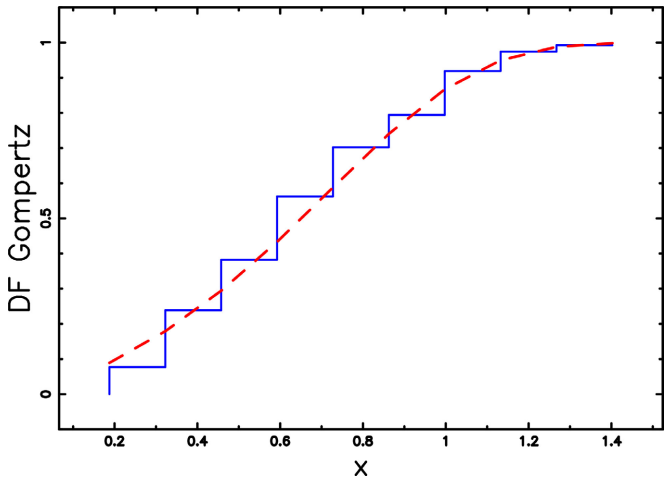

Figure 1. Empirical DF of the mass distribution for NGC 2362 (blue histogram) with a superposition of the Gompertz DF (red dashed line). Theoretical parameters as in **Table 1**.

Table 2. Numerical values of χ^2_{red}, AIC, probability Q, D, the maximum distance between theoretical and observed DFs, and P_{KS}, the significance level, in the K-S test of the truncated Gompertz distribution, see Equation (19), for different astrophysical environments. The last column (F) indicates a P_{KS} higher (Y) or lower (N) than that for the log-normal distribution. The number of linear bins, n, is 10.

Cluster	parameters	AIC	χ^2_{red}	Q	D	P_{KS}	F
NGC 2362	a = 0.525, b = 2.336	17.268	1.544	0.159	4.344×10^{-2}	0.674	Y
NGC 6611	a = 1.819, b = 0.647	12.35	12.35	0.628	7.325×10^{-2}	0.208	Y
γ Velorum	a = 3.26, b =	43.58	5.93	3.325×10^{-6}	0.173	9.261×10^{-7}	N
Berkeley 59	a = 1.2, b = 1.02	171	27.16	0	0.311	0	N

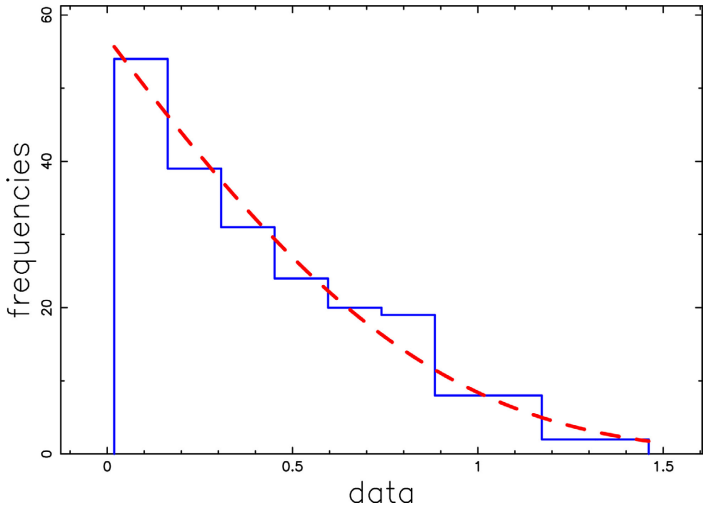

Figure 2. Empirical PDF of the mass distribution for NGC 6611 (blue histogram) with a superposition of the truncated Gompertz PDF (red dashed line). Theoretical parameters as in **Table 2**.

5. Luminosity Function for Galaxies

5.1. Processed Catalogs

The tests of the Gompertz luminosity function (LF) have been made on the u^* band of SDSS as in [20] with data available at https://cosmo.nyu.edu/blanton/lf.html. The tests on the photometric maximum and average magnitude as functions of the redshift have been made on the catalog GLADE+ that contains ≈ 22.5 million galaxies [21].

5.2. Schechter Luminosity

The Schechter function, introduced by [22], provides a useful reference for the LF of galaxies

$$\Phi\left(L;\alpha,L^*,\Phi^*\right)\mathrm{d}L=\frac{\Phi^*}{L^*}\left(\frac{L}{L^*}\right)^{\alpha}\exp\left(-\frac{L}{L^*}\right)\mathrm{d}L, \tag{34}$$

here α sets the slope for low values of L, L^* is the characteristic luminosity and Φ^* is the normalization. The equivalent distribution in absolute magni-

tude is

$$\Phi(M)\mathrm{d}M = 0.921\Phi^{*}10^{0.4(\alpha+1)\left(M^{*}-M\right)}\exp\left(-10^{0.4\left(M^{*}-M\right)}\right)\mathrm{d}M, \tag{35}$$

where M^{*} is the characteristic magnitude as derived from the data. We now introduce the parameter h, which is $H_0/100$, where H_0 is the Hubble constant. The scaling with h is $M^{*}-5\log_{10}h$ and $\Phi^{*}h^{3}\left[\mathrm{Mpc}^{-3}\right]$.

5.3. Gompertz Luminosity Function

In order to derive the Gompertz LF, we start from the PDF as given by Equation (1) and we substitute b with $\frac{1}{L^{*}}$ and x with L

$$\Psi\left(L;\alpha,\beta,L^{*},\Psi^{*}\right)\mathrm{d}L = Y^{*}a\mathrm{e}^{\frac{L}{L^{*}}-aL^{*}\left(\mathrm{e}^{\frac{L}{L^{*}}}-1\right)}\mathrm{d}L, \tag{36}$$

where L is the luminosity defined for $[0,\infty]$, L^{*} is the characteristic luminosity and Ψ^{*} is a normalization, *i.e.* the number of galaxies in a cubic Mpc. The mean luminosity, $\bar{L}$, is

$$\bar{L}\left(a,L^{*}\right) = Y^{*}L^{*}\mathrm{e}^{aL^{*}}\mathrm{Ei}_1\left(aL^{*}\right), \tag{37}$$

see formulae (A.1) for the definition of $\mathrm{Ei}_a(z)$ in the Appendix. We now introduce the following useful formulae relating the absolute magnitude and luminosity

$$\frac{L}{L_{\odot}} = 10^{0.4\left(M_{\odot}-M\right)}, \frac{L^{*}}{L_{\odot}} = 10^{0.4\left(M_{\odot}-M^{*}\right)} \tag{38}$$

where $L_{\odot}$ and $M_{\odot}$ are the luminosity and absolute magnitude of the sun in the considered band. The LF in absolute magnitude is therefore

$$\begin{aligned}&\Psi\left(M;a,M^{*},\Psi^{*}\right)\mathrm{d}M\\&= 0.4a\mathrm{e}^{-10^{-0.4M^{*}}}\mathrm{e}^{10^{-0.4M+0.4M^{*}}}a+10^{-0.4M^{*}}a+10^{-0.4M+0.4M^{*}}Y^{*}10^{-0.4M}\ln(10)\mathrm{d}M.\end{aligned} \tag{39}$$

The Schechter function, the Gompertz LF represented by formula (39) and the data are presented in **Figure 3**, parameters as in **Table 3**.

5.4. Truncated Gompertz Luminosity Function

The truncated Gompertz LF for galaxies according to Equation (19) is

$$\begin{aligned}&\Psi\left(L;a,L^{*},\Psi^{*},L_l,L_u\right)\mathrm{d}L\\&= \frac{Y^{*}a\mathrm{e}^{\frac{L}{L^{*}}-aL^{*}\left(\mathrm{e}^{\frac{L}{L^{*}}}-1\right)}}{\mathrm{e}^{-a\mathrm{e}^{\frac{L_u}{L^{*}}}L^{*}}\mathrm{e}^{a\mathrm{e}^{\frac{L_u}{L^{*}}}L^{*}}-\mathrm{e}^{-a\mathrm{e}^{\frac{L_u}{L^{*}}}L^{*}}\mathrm{e}^{aL^{*}}+\mathrm{e}^{-a\mathrm{e}^{\frac{L_l}{L^{*}}}L^{*}}\mathrm{e}^{aL^{*}}-\mathrm{e}^{-a\mathrm{e}^{\frac{L_l}{L^{*}}}L^{*}}\mathrm{e}^{a\mathrm{e}^{\frac{L_l}{L^{*}}}L^{*}}},\end{aligned} \tag{40}$$

where the random variable L is defined for $[L_l,L_u]$, L_l is the lower boundary in luminosity, L_u is the upper boundary in luminosity, L^{*} is the characteristic luminosity and Ψ^{*} is the normalization. The mean luminosity, $\bar{L}_T$, is

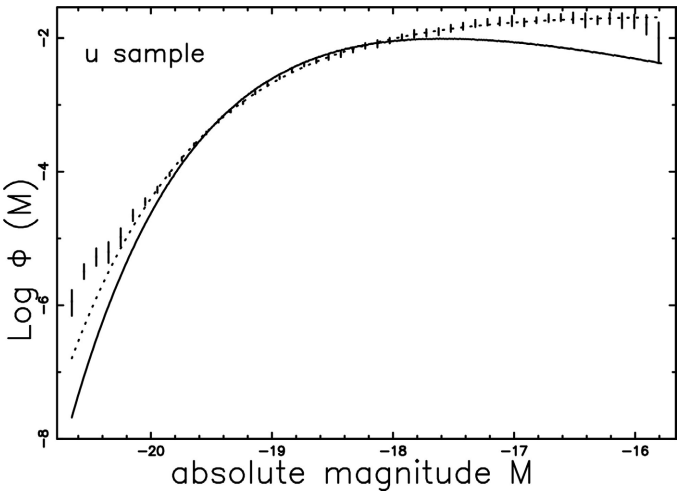

Figure 3. The LF data of SDSS(u^*) are represented with error bars. The continuous line fit represents the Gompertz LF (39) and the dotted line represents the Schechter function.

Table 3. Numerical values and χ^2_{red} of the LFs applied to SDSS Galaxies in the u^* band.

LF	parameters	χ^2_{red}
Schechter	$M^*=-17.92$, $\alpha=-0.9$, $\Phi^*=0.03/\mathrm{Mpc}^3$	0.689
Gompertz	$M^*=-30.37$, $a=9.24\times10^{-8}$, $\Psi^*=2.88\times10^{-2}/\mathrm{Mpc}^3$	6.64

$$\bar{L}_T\left(a,L^*,L_l,L_u\right)=\frac{Y^*}{\mathrm{e}^{-a\mathrm{e}^{\frac{L_u}{L^*}}L^*}\mathrm{e}^{a\mathrm{e}^{\frac{L_u}{L^*}}L^*}-\mathrm{e}^{-a\mathrm{e}^{\frac{L_u}{L^*}}L^*}\mathrm{e}^{aL^*}+\mathrm{e}^{-a\mathrm{e}^{\frac{L_l}{L^*}}L^*}\mathrm{e}^{aL^*}-\mathrm{e}^{-a\mathrm{e}^{\frac{L_l}{L^*}}L^*}\mathrm{e}^{a\mathrm{e}^{\frac{L_l}{L^*}}L^*}}$$
$$\times\left[-\left(L^*\mathrm{e}^{aL^*}\mathrm{Ei}_1\left(a\mathrm{e}^{\frac{L_u}{L^*}}L^*\right)-L^*\mathrm{e}^{aL^*}\mathrm{Ei}_1\left(a\mathrm{e}^{\frac{L_l}{L^*}}L^*\right)-L_l\mathrm{e}^{-aL^*\left(\mathrm{e}^{\frac{L_l}{L^*}}-1\right)}+L_u\mathrm{e}^{-aL^*\left(\mathrm{e}^{\frac{L_u}{L^*}}-1\right)}\right)\right]. \quad (41)$$

The magnitude version is

$$\Psi\left(M;a,M^*,\Psi^*,M_l,M_u\right)\mathrm{d}M$$
$$=\Psi^*\frac{-0.4a\mathrm{e}^{-a10^{-0.4M^*+0.4M_\odot}\left(\mathrm{e}^{10^{0.4M^*-0.4M}}-1\right)+10^{0.4M^*-0.4M}}10^{-0.4M+0.4M_\odot}\left(\ln(2)+\ln(5)\right)}{\mathrm{e}^{-10^{-0.4M^*+0.4M_\odot}a\left(\mathrm{e}^{10^{-0.4M_l+0.4M^*}}-1\right)}-\mathrm{e}^{-10^{-0.4M^*+0.4M_\odot}a\left(\mathrm{e}^{10^{-0.4M_u+0.4M^*}}-1\right)}}\mathrm{d}M, \quad (42)$$

where M is the absolute magnitude, M^* is the characteristic magnitude, M_l is the lower boundary of the magnitudes and M_u is the upper boundary of the magnitudes. The two luminosities L_l and L_u are connected with the absolute magnitudes M_l and M_u through the following relation:

$$\frac{L_l}{L_\odot}=10^{0.4(M_\odot-M_u)},\frac{L_u}{L_\odot}=10^{0.4(M_\odot-M_l)} \quad (43)$$

where the indices u and l are inverted in the transformation from luminosity to

absolute magnitude. The mean theoretical absolute magnitude, $\langle M \rangle$, can be evaluated as

$$\langle M \rangle = \frac{\int_{M_l}^{M_u} M \times \Psi\left(M; a, c, M^*, \Psi^*, M_l, M_u\right) \mathrm{d}M}{\int_{M_l}^{M_u} \Psi\left(a, M; c, M^*, \Psi^*, M_l, M_u\right) \mathrm{d}M}. \tag{44}$$

The Schechter function, the truncated Gompertz LF represented by formula (42) and the data are presented in Figure 4 with parameters as in Table 4.

5.5. The Photometric Maximum

In the pseudo-Euclidean universe, we introduce

$$z_{crit}^2 = \frac{H_0^2 L^*}{4\pi f c_l^2}, \tag{45}$$

which allows defining the joint distribution in z (redshift) and f (flux) for the Gompertz LF as

$$\frac{\mathrm{d}N}{\mathrm{d}\Omega \mathrm{d}z \mathrm{d}f} = \frac{4 z^2 c_l^5 \Psi^* a \left(\frac{z^2}{z_{crit}^2}\right)^c c\pi z_{crit}^2 \mathrm{e}^{-a\left(\frac{z^2}{z_{crit}^2}\right)^c}}{H_0^5 L^*}, \tag{46}$$

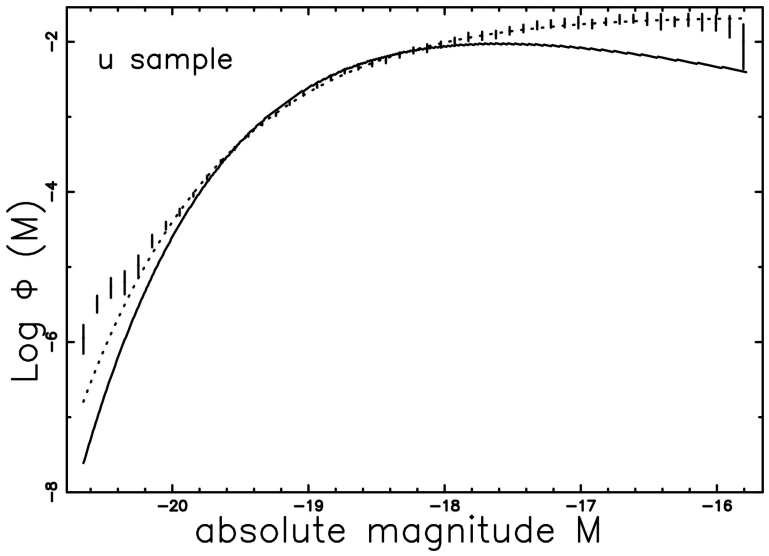

Figure 4. The LF data of SDSS (u^*) are represented with error bars. The continuous line fit represents the truncated Gompertz LF (42) and the dotted line represents the Schechter function.

Table 4. Numerical values and χ_{red}^2 of the truncated Gompertz and Schechter LFs applied to SDSS Galaxies in the u^* band.

LF	parameters	χ_{red}^2
Schechter	$M^* = -17.92$, $\alpha = -0.9$, $\Phi^* = 0.03/\mathrm{Mpc}^3$	0.689
Truncated Gompertz	$M^* = -31.41$, $a = 5.92 \times 10^{-10}$, $\Psi^* = 2.67 \times 10^{-2}/\mathrm{Mpc}^3$	6.66

where $\mathrm{d}\Omega$, $\mathrm{d}z$ and $\mathrm{d}f$ represent the differentials of the solid angle, the redshift, and the flux, respectively, L^* is the characteristic luminosity, c_l is the speed of light, and H_0 is the Hubble constant; see [23] for more details. The solution of the following non-linear equation determines a maximum at $z = z_{\max}$

$$L^* \mathrm{e}^{\frac{z^2}{z_{crit}^2}} a z^2 - z^2 - 2z_{crit}^2 = 0. \tag{47}$$

The above equation does not have an analytical solution and therefore the position in z of the maximum should evaluated numerically. A practical formula for the number of galaxies is

$$\frac{\mathrm{d}N}{\mathrm{d}\Omega \mathrm{d}z \mathrm{d}f} = \frac{1}{H_0^5}\left[Y^* 12.566 z^4 c_l^5 a \mathrm{e}^{\frac{12.566 f z^2 c_l^2}{10.0^{0.4M_\odot - 0.4aM^*} H_0^2} - 1.0 a 10.0^{0.4M_\odot - 0.4aM^*} \left(\mathrm{e}^{\frac{12.5666 f z^2 c_l^2}{10.0^{0.4M_\odot - 0.4aM^*} H_0^2}} - 1.0 \right)} \right], \tag{48}$$

and the equivalent for the Schechter LF is

$$\frac{\mathrm{d}N}{\mathrm{d}\Omega \mathrm{d}z \mathrm{d}f} = \frac{1}{H_0^5 10^{0.4M_\odot - 0.4M^*}}\left[4 z^4 c_l^5 F^* \left(\frac{4\pi f z^2 c_l^2}{H_0^2 10^{0.4M_\odot - 0.4M^*}} \right)^\alpha \mathrm{e}^{-\frac{4\pi f z^2 c_l^2}{H_0^2 10^{0.4M_\odot - 0.4M^*}}} \pi \right]. \tag{49}$$

A numerical result is presented in **Figure 5**, where we display the number of observed galaxies for the Glade+ catalog at a given apparent magnitude and both the Schechter and Gompertz models for the number of galaxies as functions of the redshift.

All the galaxies with $f_{\min} < f < f_{\max}$ are obtained by integrating Equation (48) with respect to f:

$$\frac{\mathrm{d}N}{\mathrm{d}\Omega \mathrm{d}z} = \frac{1}{H_0^3}\left[-Y^* z^2 c_l^3 \left(\mathrm{e}^{10^{0.4M_\odot - 0.4M^*} a - 10^{0.4M_\odot - 0.4M^*} a \mathrm{e}^{\frac{12.56 \times 10^{-0.4M_\odot + 0.4M^*} f_{\max} z^2 c_l^2}{H_0^2}}} - \mathrm{e}^{10^{0.4M_\odot - 0.4M^*} a - 10^{0.4M_\odot - 0.4M^*} a \mathrm{e}^{\frac{12.56 \times 10^{-0.4M_\odot + 0.4M^*} f_{\min} z^2 c_l^2}{H_0^2}}} \right) \right], \tag{50}$$

with the equivalent formula for the Schechter LF

$$\frac{\mathrm{d}N}{\mathrm{d}\Omega \mathrm{d}z} = \frac{1}{H_0^3}\left[-F^* c^3 z^2 \left(\Gamma\left(\alpha + 1, \frac{4\pi f_{\max} z^2 c^2 10^{-0.4M_\odot + 0.4M^*}}{H_0^2} \right) - \Gamma\left(\alpha + 1, \frac{4\pi f_{\min} z^2 c^2 10^{-0.4M_\odot + 0.4M^*}}{H_0^2} \right) \right) \right], \tag{51}$$

where the incomplete Gamma function is defined by Equation (A.3). All the ga-

laxies of GLADE+ are shown in Figure 6 together with the two theoretical models.

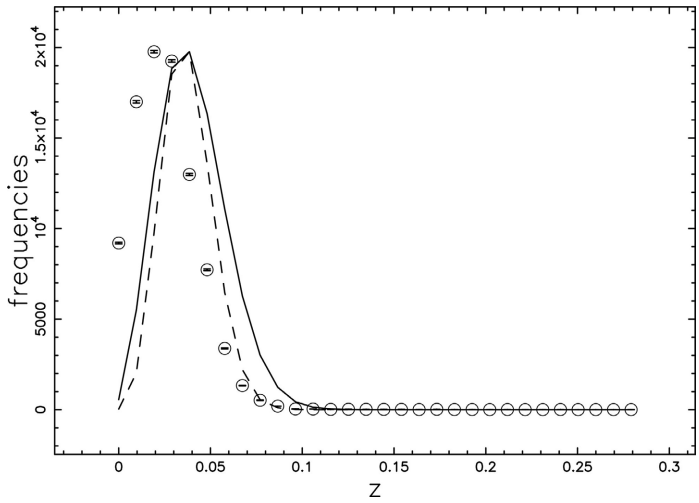

Figure 5. The galaxies of GLADE+ with $9.13 \le m \le 15.62$ or $69091 \frac{L_{\odot}}{\mathrm{Mpc}^2} \le f \le 27275154 \frac{L_{\odot}}{\mathrm{Mpc}^2}$ are organized in frequencies versus heliocentric redshift, (empty circles); the error bar is given by the square root of the frequency. The maximum frequency of observed galaxies is at $z = 0.024$. The full line is the theoretical curve generated by $\frac{\mathrm{d}N}{\mathrm{d}\Omega \mathrm{d}z \mathrm{d}f}(z)$ as given by the application of the Schechter LF which is Equation (49) and the dashed line represents the Gompertz LF which is Equation (48). The parameters for the Gompertz LF are $a = 4 \times 10^{-13}$, $M^* = -34$, $\chi^2 = 3193$ for the Schechter LF and $\chi^2 = 1393$ for the Gompertz LF.

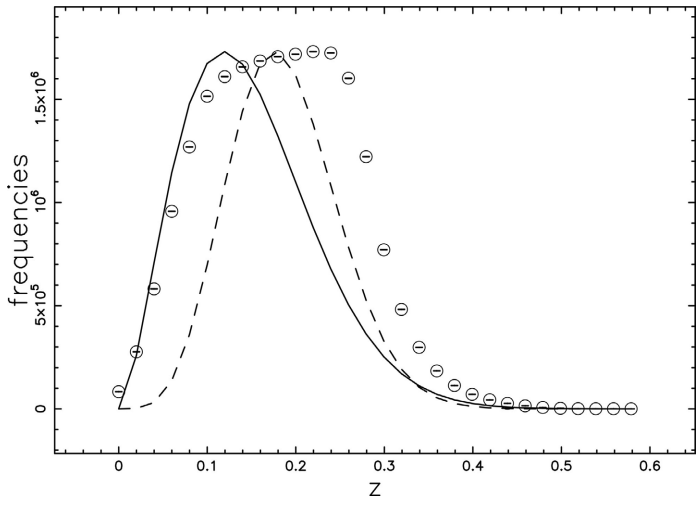

Figure 6. All the galaxies of GLADE+ are organized in frequencies versus heliocentric redshift, (empty circles); the error bar is given by the square root of the frequency. The maximum frequency of all observed galaxies is at $z = 0.219$. The full line is the theoretical curve generated by $\frac{\mathrm{d}N}{\mathrm{d}\Omega \mathrm{d}z}(z)$ as given by the application of the Schechter LF, see Equation (51), and the dashed line represents the Gompertz LF which is Equation (50). The parameters of the Gompertz LF are the same as in Figure 5.

5.6. Mean Absolute Magnitude

We review the most important equations that allow modeling the mean absolute magnitude as a function of the redshift. The absolute magnitude is

$$M_L = m_L - 5\log_{10}\left(\frac{cz}{H_0}\right) - 25, \tag{52}$$

where $m_L = 28$ for the GLADE+ catalog.

The theoretical average absolute magnitude of the truncated Gompertz LF, see Equation (44), can be compared with the observed average absolute magnitude of the GLADE+ catalog as a function of the redshift. To fit the data, we assumed the following empirical dependence on the redshift for the characteristic magnitude of the truncated Gompertz LF

$$M^* = -21 + 3\left(1 - \left(\frac{z - z_{\min}}{z_{\max} - z_{\min}}\right)^{0.6}\right), \tag{53}$$

where $z_{\min}$ and $z_{\max}$ are the minimum and the maximum value of the redshift in the considered catalog: in the case of the GLADE+ catalog $z_{\min} = 1.03 \times 10^{-4}$ and $z_{\max} = 0.6$. The lower/upper bounds in absolute magnitude are given by the minimum/maximum magnitude of the selected bin in redshift, the characteristic magnitude varies according to Equation (53) and **Figure 7** shows a comparison between the mean theoretical absolute magnitude and the observed mean absolute magnitude for the Glade+ catalog.

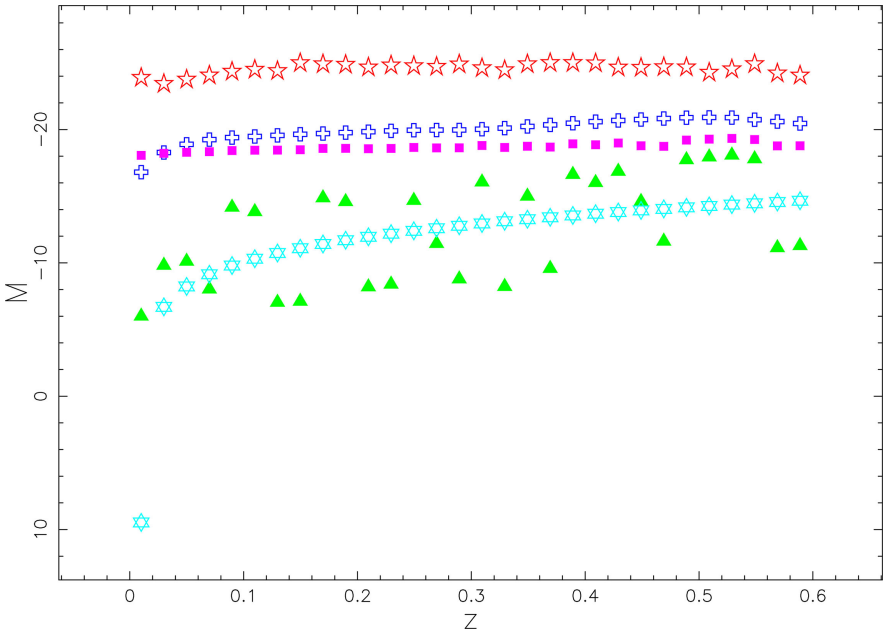

Figure 7. Observed minimum absolute magnitude (red empty stars), observed average absolute magnitude (blue empty crosses), theoretical average absolute magnitude for the truncated Gompertz LF as given by Equation (44) (magenta full squares), lower theoretical curve as represented by Equation (52) (cyan empty stars of David) and observed maximum absolute magnitude (green full triangles).

6. Conclusions

The truncated distribution

We derived the PDF, the DF, the average value, the second moment, the median, the random number generator and the MLE for the Gompertz distribution truncated on the left and the right.

Application to the IMF

The application of the Gompertz distribution to the IMF for stars gives better results than the lognormal distribution for two out of four samples, see Table 1. The truncated Gompertz distribution gives better results than the untruncated one for one of the four samples, see Table 1 and Table 2.

The results for the mass distribution of γ Velorum cluster compared with other distributions are shown in Table 5, in which the truncated Gompertz distribution occupies the last position.

Gompertz luminosity function

The Gompertz LF in the absolute magnitude version is derived using the standard and the truncated DFs, see formulae (39) and (42). The application to SDSS Galaxies gives a bigger reduced merit function than that from using the Schechter LF, see Table 3 and Table 4.

Cosmological applications

The maximum number of galaxies for a given solid angle as a function of the redshift which is visible in the catalog GLADE+ can be modeled with the Gompertz LF in the case of a selected flux or apparent magnitude, see Figure 5 and in the case of all galaxies, see Figure 6.

Table 5. Numerical values of D, the maximum distance between theoretical and observed DF, and P_{KS}, the significance level, in the K-S test for different distributions in the case of γ Velorum cluster.

Distribution	Reference	D	P_{KS}
truncated Gompertz	here	0.173	9.27×10^{-7}
truncated Topp-Leone	[24]	6.09×10^{-2}	0.25
Frècet	[25]	0.125	3.13×10^{-4}
truncated Frècet	[25]	0.077	0.07
truncated Weibull	[23]	0.046	0.576
truncated Sujatha	[26]	0.0485	0.534
truncated Lindley	[27]	0.11	0.48
generalized gamma	[28]	0.11	1.24×10^{-3}
truncated generalized gamma	[28]	0.062	0.24
lognormal	[29]	0.0729	0.11
truncated lognormal	[29]	0.047	0.55
gamma	[30]	0.059	0.28
truncated gamma	[30]	0.0754	0.08
beta	[31]	0.059	0.28

The average absolute magnitude of the GLADE+ galaxies as a function of the redshift, can be theoretically modeled with the truncated Gompertz LF, see Figure 7.

Conflicts of Interest

The author declares no conflicts of interest regarding the publication of this paper.

References

[1] Gompertz, B. (1825) On the Nature of the Function Expressive of the Law of Human Mortality, and on a New Mode of Determining the Value of Life Contingencies. In a Letter to Francis Baily, Esq. F.R.S. &c. *Philosophical Transactions of the Royal Society of London*, **115**, 513-583. https://doi.org/10.1098/rstl.1825.0026

[2] Aggarwal, R. and Kaur, M. (2020) Compelling Evidence of Oscillatory Behaviour of Hadronic Multiplicities in the Shifted Gompertz Distribution. *Advances in High Energy Physics*, **2020**, Article ID: 5464682. https://doi.org/10.1155/2020/5464682

[3] Chawla, R. and Kaur, M. (2018) A New Distribution for Multiplicities in Leptonic and Hadronic Collisions at High Energies. *Advances in High Energy Physics*, **2018**, Article ID: 5129341. https://doi.org/10.1155/2018/5129341

[4] Singla, A. and Kaur, M. (2020) Charged-Particle Multiplicity Moments as Described by Shifted Gompertz Distribution in e^+e^-, $p\overline{p}$, and pp Collisions at High Energies. *Advances in High Energy Physics*, **2020**, Article ID: 5192193.

[5] Sharma, R., Aggarwal, R. and Kaur, M. (2023) Statistical Analysis of Neutrino-Induced Hadron Production from a Different Perspective. *Physical Review D*, **108**, Article 113011. https://doi.org/10.1103/physrevd.108.113011

[6] Lenart, A. (2012) The Gompertz Distribution and Maximum Likelihood Estimation of Its Parameters: A Revision. MPDIR Work Paper-2012-008, Max Planck Institute for Demographic Research, Rostock, 19 p. https://doi.org/10.4054/MPIDR-WP-2012-008

[7] Lenart, A. (2012) The Moments of the Gompertz Distribution and Maximum Likelihood Estimation of Its Parameters. *Scandinavian Actuarial Journal*, **2014**, 255-277. https://doi.org/10.1080/03461238.2012.687697

[8] Press, W.H., Teukolsky, S.A., Vetterling, W.T. and Flannery, B.P. (1992) Numerical Recipes in FORTRAN. The Art of Scientific Computing. Cambridge University Press, Cambridge.

[9] Akaike, H. (1974) A New Look at the Statistical Model Identification. *IEEE Transactions on Automatic Control*, **19**, 716-723. https://doi.org/10.1109/tac.1974.1100705

[10] Liddle, A.R. (2004) How Many Cosmological Parameters? *Monthly Notices of the Royal Astronomical Society*, **351**, L49-L53. https://doi.org/10.1111/j.1365-2966.2004.08033.x

[11] Godlowski, W. and Szydowski, M. (2005) Constraints on Dark Energy Models from Supernovae. 1604-2004: *Supernovae as Cosmological Lighthouses*, Vol. 342, Padua, 15-19 June 2004, 508-516.

[12] Kolmogoroff, A. (1941) Confidence Limits for an Unknown Distribution Function. *The Annals of Mathematical Statistics*, **12**, 461-463. https://doi.org/10.1214/aoms/1177731684

[13] Smirnov, N. (1948) Table for Estimating the Goodness of Fit of Empirical Distributions. *The Annals of Mathematical Statistics*, **19**, 279-281. https://doi.org/10.1214/aoms/1177730256

[14] Massey, F.J. (1951) The Kolmogorov-Smirnov Test for Goodness of Fit. *Journal of the American Statistical Association*, **46**, 68-78. https://doi.org/10.1080/01621459.1951.10500769

[15] Irwin, J., Hodgkin, S., Aigrain, S., Bouvier, J., Hebb, L., Irwin, M., *et al.* (2008) The Monitor Project: Rotation of Low-Mass Stars in NGC 2362-Testing the Disc Regulation Paradigm at 5 Myr. *Monthly Notices of the Royal Astronomical Society*, **384**, 675-686. https://doi.org/10.1111/j.1365-2966.2007.12725.x

[16] Moitinho, A., Alves, J., Huélamo, N. and Lada, C.J. (2001) NGC 2362: A Template for Early Stellar Evolution. *The Astrophysical Journal*, **563**, L73-L76. https://doi.org/10.1086/338503

[17] Oliveira, J.M., Jeffries, R.D. and Van Loon, J.T. (2009) The Low-Mass Initial Mass Function in the Young Cluster NGC 6611. *Monthly Notices of the Royal Astronomical Society*, **392**, 1034-1050. https://doi.org/10.1111/j.1365-2966.2008.14140.x

[18] Prisinzano, L., Damiani, F., Micela, G., Jeffries, R.D., Franciosini, E., Sacco, G.G., *et al.* (2016) The *Gaia*-ESO Survey: Membership and Initial Mass Function of the γ Velorum Cluster. *Astronomy & Astrophysics*, **589**, Article No. A70. https://doi.org/10.1051/0004-6361/201527875

[19] Panwar, N., Pandey, A.K., Samal, M.R., Battinelli, P., Ogura, K., Ojha, D.K., *et al.* (2018) Young Cluster Berkeley 59: Properties, Evolution, and Star Formation. *The Astronomical Journal*, **155**, Article 44. https://doi.org/10.3847/1538-3881/aa9f1b

[20] Blanton, M.R., Hogg, D.W., Bahcall, N.A., Brinkmann, J., Britton, M., Connolly, A.J., *et al.* (2003) The Galaxy Luminosity Function and Luminosity Density at Redshift $z = 0.1$. *The Astrophysical Journal*, **592**, 819-838. https://doi.org/10.1086/375776

[21] Dálya, G., Díaz, R., Bouchet, F.R., Frei, Z., Jasche, J., Lavaux, G., *et al.* (2022) GLADE+: An Extended Galaxy Catalogue for Multimessenger Searches with Advanced Gravitational-Wave Detectors. *Monthly Notices of the Royal Astronomical Society*, **514**, 1403-1411. https://doi.org/10.1093/mnras/stac1443

[22] Schechter, P. (1976) An Analytic Expression for the Luminosity Function for Galaxies. *The Astrophysical Journal*, **203**, 297-306. https://doi.org/10.1086/154079

[23] Zaninetti, L. (2021) New Probability Distributions in Astrophysics: V. The Truncated Weibull Distribution. *International Journal of Astronomy and Astrophysics*, **11**, 133-149. https://doi.org/10.4236/ijaa.2021.111008

[24] Zaninetti, L. (2023) New Probability Distributions in Astrophysics: XI. Left Truncation for the Topp-Leone Distribution. *International Journal of Astronomy and Astrophysics*, **13**, 154-165. https://doi.org/10.4236/ijaa.2023.133009

[25] Zaninetti, L. (2022) New Probability Distributions in Astrophysics: X. Truncation and Mass-Luminosity Relationship for the Frèchet Distribution. *International Journal of Astronomy and Astrophysics*, **12**, 347-362. https://doi.org/10.4236/ijaa.2022.124020

[26] Zaninetti, L. (2021) New Probability Distributions in Astrophysics: VI. The Truncated Sujatha Distribution. *International Journal of Astronomy and Astrophysics*, **11**, 517-529. https://doi.org/10.4236/ijaa.2021.114028

[27] Zaninetti, L. (2020) New Probability Distributions in Astrophysics: II. The Generalized and Double Truncated Lindley. *International Journal of Astronomy and Astrophysics*, **10**, 39-55. https://doi.org/10.4236/ijaa.2020.101004

[28] Zaninetti, L. (2019) New Probability Distributions in Astrophysics: I. The Truncated Generalized Gamma. *International Journal of Astronomy and Astrophysics*, **9**, 393-410. https://doi.org/10.4236/ijaa.2019.94027

[29] Zaninetti, L. (2017) A Left and Right Truncated Lognormal Distribution for the Stars. *Advances in Astrophysics*, **2**, 197-213. https://doi.org/10.22606/adap.2017.23005

[30] Zaninetti, L. (2013) A Right and Left Truncated Gamma Distribution with Application to the Stars. *Advanced Studies in Theoretical Physics*, **7**, 1139-1147. https://doi.org/10.12988/astp.2013.310125

[31] Zaninetti, L. (2013) The Initial Mass Function Modeled by a Left Truncated Beta Distribution. *The Astrophysical Journal*, **765**, Article 128. https://doi.org/10.1088/0004-637x/765/2/128

[32] Olver, F.W.J., Lozier, D.W., Boisvert, R.F. and Clark, C.W. (2010) NIST Handbook of Mathematical Functions. Cambridge University Press, Cambridge.

Appendix A. Useful Power Series

The exponential integral [32] is defined for $0 < \Re(z)$.

$$\mathrm{Ei}_a(z) = \int_1^\infty \mathrm{e}^{-yz} y^{-a} \mathrm{d}y, \tag{A.1}$$

and in the case $a = 1$ has the following power series

$$\mathrm{Ei}_1(z) = -\gamma - \ln(x) + \sum_{n=0}^{\infty} \frac{(-1)^n x^{n+1}}{(n+1)(n+1)!}. \tag{A.2}$$

The incomplete Gamma function is defined by

$$\Gamma(a,z) = \int_z^\infty t^{a-1} \mathrm{e}^{-t} \mathrm{d}t, \tag{A.3}$$

and has the following power series

$$\Gamma(a,z) = \sum_{n=0}^{\infty} \left(-\frac{z^a (-z)^n}{\Gamma(n+1)(n+a)} \right) + \Gamma(a), \tag{A.4}$$

see [32] for more details.

The generalized hypergeometric function is defined by

$$pFq(n,d,z) = \sum_{k=0}^{\infty} \frac{z^k \left(\prod_{i=1}^{p} (n_i)_k \right)}{k! \left(\prod_{j=1}^{q} (d_j)_k \right)}, \tag{A.5}$$

where the Pochhammer symbol pochhammer (z, a) is

$$\mathrm{pochhammer}(z,a) = (z)_a = \frac{\Gamma(z+a)}{\Gamma(z)}. \tag{A.6}$$

We now present the series expansion of some particular cases of the generalized hypergeometric function

$${}_3F_3(1,1,1;2,2,2;z) = \sum_{n=0}^{\infty} \frac{z^n}{(n+1)^2 (n+1)!}, \tag{A.7}$$

$$ {}_4F_4\left(1,1,1,1;2,2,2,2;z\right)=\sum_{n=0}^{\infty}\frac{z^n}{\left(n+1\right)^3\left(n+1\right)!}, \tag{A.8}$$

$$ {}_5F_5\left(1,1,1,1,1;2,2,2,2,2;z\right)=\sum_{n=0}^{\infty}\frac{z^n}{\left(n+1\right)^4\left(n+1\right)!}. \tag{A.9}$$

The Euler-Mascheroni constant is defined by

$$ \gamma=\lim_{n\to\infty}\sum_{k=1}^{n}\left(\frac{1}{k}-\ln\left(1+\frac{1}{k}\right)\right)\approx 0.5772156649. \tag{A.10}$$

The Riemann zeta function is

$$ \zeta\left(z\right)=\sum_{i=1}^{\infty}\frac{1}{i^z}. \tag{A.11}$$